

LA-9053-MS

C.3

Los Alamos National Laboratory is operated by the University of California for the United States Department of Energy under contract W-7405-ENG-36.



PBX 9502 Performance

Los Alamos Los Alamos National Laboratory
Los Alamos, New Mexico 87545

DISCLAIMER

This report was prepared as an account of work sponsored by an agency of the United States Government. Neither the United States Government nor any agency thereof, nor any of their employees, makes any warranty, express or implied, or assumes any legal liability or responsibility for the accuracy, completeness, or usefulness of any information, apparatus, product, or process disclosed, or represents that its use would not infringe privately owned rights. References herein to any specific commercial product, process, or service by trade name, trademark, manufacturer, or otherwise, does not necessarily constitute or imply its endorsement, recommendation, or favoring by the United States Government or any agency thereof. The views and opinions of authors expressed herein do not necessarily state or reflect those of the United States Government or any agency thereof.

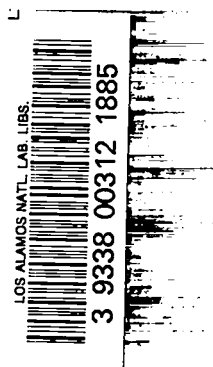
LA-9053-MS

UC-45

Issued: October 1981

PBX 9502 Performance

Charles L. Mader
M. S. Shaw
John B. Ramsay



Los Alamos Los Alamos National Laboratory
Los Alamos, New Mexico 87545

PBX 9502 PERFORMANCE

by

Charles L. Mader, M. S. Shaw, and John B. Ramsay

ABSTRACT

The performance of PBX 9502 may be described using the BKW equation of state and the multiple-shock Forest Fire model.

I. INTRODUCTION

PBX 9502 is an insensitive high explosive consisting of 95 wt% TATB (tri-amino trinitrobenzene) and 5 wt% Kel-F binder. The C-J BKW-calculated performance at 1.894 g/cm^3 is 285 kbar and 7707 m/s. The BKW-isentrope and Forest Fire rate is identical to that of X0290 given in Ref. 1. The gamma-law isentrope is given in Table I.

As described in Ref. 1, the failure diameter and detonation wave corner-turning properties of PBX 9502 can be modeled using the BKW equation of state and Forest Fire burn rates. In Ref. 2 we modeled the observed desensitization of PBX 9502 by preshocking using a Forest Fire decomposition rate determined only by the initial shock pressure of the first shock wave passing through the explosive. This is called the multiple-shock Forest Fire or MSFF model.

In Ref. 3 the Los Alamos gap test data for PBX 9502 were numerically modeled using the BKW equation-of-state data and Forest Fire kinetics. In Ref. 4 the same model was used to model the initiation of PBX 9502 by jets of copper, aluminum, and water. In Ref. 5 the initiation of detonation in PBX 9502 by triple-wave interactions was modeled.

In Ref. 6 the initiation of propagating detonation in PBX 9502 by hemispherical initiators was described numerically and the calculated large regions of partially decomposed explosive agreed with experimental observations of Travis.

This impressive list of successfully modeled PBX 9502 experiments could not be used to evaluate the adequacy of the PBX 9502 equation of state or the Forest Fire burn rates where details of the explosive performance are important.

The objective of this study to characterize PBX 9502 performance was to determine if PBX 9502 exhibited explosive performance significantly different than predicted using the BKW or gamma-law equation of state and the Forest Fire heterogeneous shock-initiation model. The study was designed to determine (1) if PBX-9502 exhibited detonation pressure buildup with run (such as exhibited by PBX 9404), (2) if the BKW or gamma-law PBX 9502 isentrope was adequate to describe the explosive behavior in the aquarium test, (3) if the Forest Fire model was adequate to describe the energy delivered by shocked but not detonated PBX 9502,

TABLE I

GAMMA-LAW CALCULATION FOR PBX 9502

GAMMA IS 2.9473500000E+00 C-J PRESSURE IS 2.4500000000E-01 DENSITY IS 1.8440000000E+00
 DETONATION VELOCITY IS 7.7070000000E-01 DLND/DLN(RHO) IS 6.6000000000E-01 Z-CONSTANT ADDED TO ENERGY IS 1.0000000000E-01
 COMPUTED ALPHA IS 2.6400500000E+00 BETA IS 1.2370000000E+00 ENERGY CONSTANT IS 6.13641141053E-02
 LNT = 0 + -0.00367771657E-01 LNW AND PV TO GAMMA IS 1.0330000000E-02
 LN(P) = -3.99074095454E+00 -2.9473500000E+00PLNV
 LN(E) = -1.63121712222E+00 4.0000000000E-01LNP 7.8521000000E-02LNP*2 5.5000000000E-03LNP*3 1.44374412574E-04LNP*4

PRESSURE (MBAARS)	VOLUME (CC/GM)	ENERGY (MB-CC/GM)	FIT ENERGY	PARTICLE VELOCITY (CM/USEC)
8.71821515024E-01	2.69770000163E-01	1.02130200000E-01	1.03200000000E-01	1.95240022621E-01
7.80105665930E-01	2.82070001161E-01	1.71485970000E-01	1.71958641021E-01	2.37245354574E-01
6.59222310203E-01	2.96007122307E-01	1.61772400793E-01	1.61799029123E-01	2.76261100272E-01
5.73236798037E-01	3.11011112706E-01	1.02915717347E-01	1.52667022346E-01	3.12504192000E-01
4.900066781250E-01	3.26110477413E-01	1.00000000000E-01	1.44442310001E-01	3.46171652113E-01
4.33449375000E-01	3.41951000000E-01	1.37477020000E-01	1.37020000000E-01	3.77000000000E-01
3.76912500000E-01	3.50556000000E-01	1.30763327737E-01	1.30310270256E-01	4.00000000000E-01
3.27750000000E-01	3.75960021033E-01	1.24641022325E-01	1.24234900000E-01	4.00000000000E-01
2.85000000000E-01	3.94220700527E-01	1.19000000000E-01	1.18724034572E-01	4.00000000000E-01
2.20000000000E-01	4.25232030206E-01	1.11512700000E-01	1.10952645315E-01	4.00000000000E-01
1.82400000000E-01	4.50676001019E-01	1.00000000000E-01	1.00000000000E-01	4.00000000000E-01
1.45920000000E-01	4.94751000000E-01	9.00000000000E-02	9.00000000000E-02	4.00000000000E-01
1.16730000000E-01	5.33663690000E-01	9.33551600000E-02	9.33551600000E-02	4.00000000000E-01
9.33000000000E-02	5.75636120000E-01	8.00000000000E-02	8.00000000000E-02	4.00000000000E-01
7.47110000000E-02	6.20000000000E-01	8.51856100000E-02	8.51856100000E-02	4.00000000000E-01
5.97600320000E-02	6.69743000000E-01	8.19201500000E-02	8.19201500000E-02	4.00000000000E-01
4.78150656000E-02	7.22410000000E-01	7.00000000000E-02	7.00000000000E-02	4.00000000000E-01
3.02520524000E-02	7.79237000000E-01	7.66707702300E-02	7.66707702300E-02	4.00000000000E-01
3.00016419000E-02	8.40523740000E-01	7.45725200000E-02	7.45725200000E-02	4.00000000000E-01
2.44813135000E-02	9.06630600000E-01	7.27619100000E-02	7.27619100000E-02	4.00000000000E-01
1.95050500000E-02	9.77936741713E-01	7.11990000000E-02	7.11990000000E-02	4.00000000000E-01
1.56680000000E-02	1.05405100000E-01	6.90512631238E-02	6.90512631238E-02	4.00000000000E-01
1.25344325566E-02	1.13700000000E-01	6.80000000000E-02	6.80000000000E-02	4.00000000000E-01
1.00275460000E-02	1.22730000000E-01	6.70000000000E-02	6.70000000000E-02	4.00000000000E-01
8.02203600000E-03	1.32380000000E-01	6.60000000000E-02	6.60000000000E-02	4.00000000000E-01
6.01762946000E-03	1.42790000000E-01	6.50000000000E-02	6.50000000000E-02	4.00000000000E-01
5.13410357520E-03	1.54025000000E-01	6.40000000000E-02	6.40000000000E-02	4.00000000000E-01
4.10720200000E-03	1.66139720000E-01	6.30000000000E-02	6.30000000000E-02	4.00000000000E-01
3.08502620000E-03	1.79200000000E-01	6.20000000000E-02	6.20000000000E-02	4.00000000000E-01
2.62866103000E-03	1.93300000000E-01	6.10000000000E-02	6.10000000000E-02	4.00000000000E-01
2.10292802440E-03	2.08500000000E-01	6.00000000000E-02	6.00000000000E-02	4.00000000000E-01
1.60234305952E-03	2.24900000000E-01	6.00000000000E-02	6.00000000000E-02	4.00000000000E-01
1.30587444762E-03	2.42500000000E-01	6.00000000000E-02	6.00000000000E-02	4.00000000000E-01
1.07669955000E-03	2.61671130000E-01	6.00000000000E-02	6.00000000000E-02	4.00000000000E-01
8.61350646475E-04	2.82251000000E-01	6.00000000000E-02	6.00000000000E-02	4.00000000000E-01
6.80000000000E-04	3.04450000000E-01	6.00000000000E-02	6.00000000000E-02	4.00000000000E-01
5.51270173744E-04	3.28300000000E-01	6.00000000000E-02	6.00000000000E-02	4.00000000000E-01
4.01016138000E-04	3.54223000000E-01	6.00000000000E-02	6.00000000000E-02	4.00000000000E-01
3.52012911190E-04	3.82000000000E-01	6.00000000000E-02	6.00000000000E-02	4.00000000000E-01
2.82250328057E-04	4.12133710000E-01	6.00000000000E-02	6.00000000000E-02	4.00000000000E-01
2.25000000000E-04	4.44547000000E-01	6.00000000000E-02	6.00000000000E-02	4.00000000000E-01
1.806400211063E-04	4.79511300000E-01	6.00000000000E-02	6.00000000000E-02	4.00000000000E-01
1.44512168420E-04	5.17224700000E-01	6.00000000000E-02	6.00000000000E-02	4.00000000000E-01
1.15609734741E-04	5.57900000000E-01	6.00000000000E-02	6.00000000000E-02	4.00000000000E-01

and (4) if the explosive performance of PBX 9502 in diverging geometry was adequately described.

II. PBX 9502 DETONATION PRESSURE BUILDUP

A series of experiments were designed to investigate the change of C-J pressure of PBX 9502 as a function of distance of run. A driver was designed such that the input shock in the PBX 9502 results in a short distance of run to detonation without overdriving the PBX 9502. The driver was a P-81 lens, 51.0 mm of Comp. B-3, and 6.3 mm of Dural. It sends a shock of about 215 kbar into the PBX 9502 with a distance of run to detonation of about 2.4 mm. The driver initiated 12.5-, 25.0-, and 50.0-mm-thick slabs of PBX 9502, which then shocked Dural plates of various thicknesses. The geometry is sketched in Fig. 1. The data are shown in Table II.

If buildup of detonation pressure as a function of distance of run is not significant, the initial free surface of the Dural plates should scale as a function of Dural plate to PBX 9502 thickness. As shown in Fig. 2, the data appear to scale and no evidence of buildup of detonation pressure as a function of run distance was observed. The calculated curves were calculated using the HYDROX one-dimensional reactive hydrodynamics code.

III. PBX 9502 AQUARIUM TEST

An aquarium test was conducted by S. Goldstein and calculated by J. N. Johnson using the 2DL hydrodynamics code. The test has been described in Ref. 7. An underwater, cylindrical, 17.78-mm-diam charge was detonated at one end and several photographic exposures were taken with the I²C camera of the expanding gas bubble behind the detonation front and the shock wave in the water. The measured detonation velocity was 7790 m/s.

The two-dimensional calculations were performed with the BKW equation of state and with a gamma-law equation of state through the BKW C-J state. The calculated and experimental bubble and shock positions defined by the 1-kbar isobar are shown in Fig. 3 for the BKW and Fig. 4 for the gamma-law isentrope. The agreement between the computed and measured shock front and bubble positions is very good, indicating the adequacy of the equation-of-state description.

IV. ENERGY DEPOSITION FROM SHOCKED PBX 9502

A series of experiments were performed to study the rate of energy delivered to a 2.5-mm magnesium plate by 4.52, 7.57, 10.51, 17.50, and 49.97 mm of PBX 9502 initially shocked to 135 kbar by a driver system. The run to detonation is about 10 mm. The driver system used was a P-80, 51 mm Comp. B-3, and 25 mm of stainless steel (type 304).

The MSFF model is necessary to reproduce the experimental data and the Pop plot. The first 10 mm of explosive continues to decompose in the MSFF model, whereas it completely reacts after detonation occurs in the Forest Fire model.

The experimental configuration is shown in Fig. 5 and the magnesium plate velocity as a function of time is shown in Figs. 6-10. The PBX 9502 used in these experiments had a slightly different Pop plot so the Forest Fire rate used is given in Table III.

TABLE II

PBX 9502 DETONATION PRESSURE DATA

Shot No.	HE		Dural (mm)	Dural/HE	U_{fs} (mm/ μ s)	Standard Deviation (mm/ μ s)
	Density (g/cm ³)	Thickness (mm)				
Nominal 12.5-mm PBX 9502						
E4829	1.887	12.51	3.20	0.256	2.999	0.0600
E4823	1.889	12.48	4.42	0.354	2.961	0.0049
E4828 ^a	1.886	12.47	6.28 ^b	0.504	2.691	0.0428
E4822	1.889	12.48	6.32	0.506	2.858	0.0475
E4821	1.888	12.48	12.55	1.006	2.443	0.0739
Nominal 25-mm PBX 9502						
E4866	1.888	25.00	3.05 ^b	0.122	3.187	0.0110
E4832	1.885	24.98	3.19	0.128	3.123	0.0501
E4831	1.890	24.99	6.31	0.253	2.935	0.0123
E4830	1.889	24.99	12.55	0.502	2.790	0.0175
E4865	1.891	24.97	12.53	0.502	2.745	0.0474
E4864	1.891	25.00	24.96 ^b	0.998	2.533	0.0416
Nominal 50-mm PBX 9502						
E4861	1.889	49.98	6.32 ^b	0.126	3.162	0.0650
E4867	1.889	49.95	6.36 ^c	0.127	3.132	0.0300
E4834	1.889	49.99	12.56	0.251	2.890	0.0127
E4833	1.887	49.97	25.03	0.501	2.708	0.0146
E4907	1.890	49.96	50.55	1.012	2.413	0.0114

^aValue rejected because of a possible error in recording the Dural plate thickness.

^bDural surface finished on air-bearing lathe with a diamond knife.

^cVapor-plated copper surface (0.02-mm-thick copper).

V. ENERGY FROM DIVERGING PBX 9502 DETONATIONS

To determine if we can model the performance of diverging detonations in PBX 9502, a 1.524-mm Dural plate was driven by a diverging PBX 9502 detonation (which ran 7.0 mm on the detonation axis) initiated by a 16-mm-radius X0351 hemispheric initiator identical to that described in Ref. 6. The system was backed by a 6.35-mm-thick steel plate.

TABLE III

PBX 9502 FOREST FIRE RATE USED IN ENERGY DEPOSITION STUDY

X0290A X0290, PCJ=0.285, DCJ = 0.7707 1OCT80 RHO = 1.89400

POP PLOT, LN(RUN) = A1 + A2*LN(P-A3), A1 = -5.942871E+00 A2 = -2.923379E+00 A3 = 0.

REACTION HUGONIOT, US = C + S*UP, C = 2.400000E-01 S = 2.500000E+00

CJ DETONATION PRESSURE = 2.850000E+01

PM1= 0. PM2= 0.

HOM EQUATION OF STATE CONSTANTS

X0290

UNREACTED EXPLOSIVE

2.400000000000E+01 2.050000000000E+00 0.
 0. -2.37141685560E+01 -1.36319013778E+02 -2.35068216661E+02
 -1.71049590083E+02 -4.22635505569E+01 1.500000000000E+00 3.000000000000E-01
 5.27983104541E+01 5.000000000000E-05 0.
 3.000000000000E+02 0. 0.
 0. 0. 0.

DETONATION PRODUCTS

-3.87828541159E+00 -2.69032297231E+00 2.22074184951E-01 7.42482128000E-02
 -3.42819430727E-02 -1.58889615377E+00 5.34895448385E-01 9.42824251124E-02
 8.25643459024E-03 2.89357822582E-04 7.06740292649E+00 -5.67003244430E-01
 5.17941586095E-02 9.84863946395E-03 -1.09218419748E-02 5.000000000000E-01
 1.000000000000E-01

X0290A X0290, PCJ=0.285, DCJ = 0.7707 1OCT80 RHO = 1.89400

POP PLOT, LN(RUN) = A1 + A2*LN(P-A3), A1 = -5.942871E+00 A2 = -2.923379E+00 A3 = 0.

REACTION HUGONIOT, US = C + S*UP, C = 2.400000E-01 S = 2.500000E+00

RUN	P	V	UP	US	W	RATE	TEMPERATURE	TIME
16.68967	.05000	.44239	.06542	.40355	.97069	3.1035E-03	479.97186	37.35853
14.47116	.05250	.44062	.06772	.40931	.96839	3.8405E-03	492.44426	31.89875
12.63110	.05500	.43894	.06998	.41495	.96604	4.7090E-03	505.11963	27.43309
11.09187	.05750	.43733	.07220	.42150	.96363	5.7252E-03	517.96687	23.74761
9.79424	.06000	.43579	.07437	.42594	.96116	6.9074E-03	530.98558	20.68097
8.69247	.06250	.43431	.07651	.43128	.95864	8.2753E-03	544.16574	18.10997
7.75083	.06500	.43290	.07862	.43654	.95606	9.8500E-03	557.49817	15.93953
6.94117	.06750	.43154	.08068	.44171	.95344	1.1654E-02	570.97452	14.09547
6.24108	.07000	.43023	.08272	.44680	.95075	1.3713E-02	584.58710	12.51939
5.63259	.07250	.42898	.08472	.45181	.94801	1.6053E-02	598.32887	11.16491
5.10113	.07500	.42776	.08670	.45674	.94522	1.8702E-02	612.19333	9.99487
4.63485	.07750	.42659	.08864	.46161	.94237	2.1692E-02	626.17450	8.97930
4.22404	.08000	.42546	.09056	.46641	.93947	2.5055E-02	640.26687	8.09384

TABLE III (cont)

X0290A X0290, PCJ=0.285, DCJ = 0.7707 10CT80 RHO = 1.89400
 POP PLOT, LN(RUN) = A1 + A2*LN(P-A3), A1 = -5.942871E+00 A2 = -2.923379E+00 A3 = 0.
 REACTION HUGONIOT, US = C + S*UP, C = 2.400000E-01 S = 2.500000E+00

RUN	P	V	UP	US	W	RATE	TEMPERATURE	TIME
3.86064	.08250	.42437	.09245	.47114	.93650	2.8027E-02	654.46531	7.31856
3.53000	.08500	.42332	.09432	.47580	.93349	3.3046E-02	668.76508	6.63706
3.25054	.08750	.42230	.09616	.48041	.93041	3.7754E-02	683.16177	6.03575
2.99387	.09000	.42131	.09798	.48496	.92728	4.2993E-02	697.65128	5.50333
2.76314	.09250	.42035	.09978	.48945	.92408	4.8810E-02	712.22977	5.03034
2.55591	.09500	.41942	.10156	.49389	.92083	5.5257E-02	726.89367	4.60882
2.36901	.09750	.41851	.10331	.49828	.91751	6.2386E-02	741.63961	4.23204
2.20000	.10000	.41763	.10505	.50262	.91414	7.0256E-02	756.46446	3.89431
2.04679	.10250	.41678	.10676	.50691	.91069	7.8928E-02	771.36526	3.59075
1.90756	.10500	.41595	.10846	.51115	.90719	8.8468E-02	786.33921	3.31722
1.78075	.10750	.41514	.11014	.51534	.90362	9.8946E-02	801.38370	3.07014
1.66501	.11000	.41436	.11180	.51949	.89998	1.1044E-01	816.49624	2.84642
1.55914	.11250	.41359	.11344	.52360	.89627	1.2301E-01	831.68987	2.64342
1.46211	.11500	.41285	.11507	.52767	.89249	1.3678E-01	846.92896	2.45882
1.37302	.11750	.41212	.11668	.53170	.88864	1.5182E-01	862.22978	2.29061
1.29106	.12000	.41141	.11827	.53569	.88472	1.6824E-01	877.59026	2.13703
1.21554	.12250	.41072	.11985	.53964	.88073	1.8614E-01	893.00843	1.99656
1.14582	.12500	.41004	.12142	.54355	.87666	2.0563E-01	908.48242	1.86784
1.08138	.12750	.40938	.12297	.54743	.87251	2.2683E-01	924.01044	1.74969
1.02170	.13000	.40873	.12451	.55127	.86828	2.4989E-01	939.59077	1.64105
.96636	.13250	.40810	.12603	.55508	.86397	2.7493E-01	955.22175	1.54101
.91497	.13500	.40749	.12754	.55886	.85957	3.0210E-01	970.90182	1.44874
.86718	.13750	.40688	.12904	.56260	.85509	3.3157E-01	986.62945	1.36351
.82269	.14000	.40629	.13052	.56631	.85051	3.6352E-01	1002.40316	1.28468
.78120	.14250	.40571	.13200	.56999	.84585	3.9812E-01	1018.22154	1.21160
.74248	.14500	.40515	.13346	.57365	.84109	4.3557E-01	1034.08322	1.14393
.70628	.14750	.40459	.13491	.57727	.83624	4.7610E-01	1049.98687	1.08104
.67242	.15000	.40405	.13634	.58086	.83129	5.1993E-01	1065.93119	1.02255
.64070	.15250	.40352	.13777	.58443	.82623	5.6731E-01	1081.91494	.96811
.61096	.15500	.40300	.13919	.58797	.82107	6.1851E-01	1097.93689	.91737
.58304	.15750	.40248	.14059	.59148	.81580	6.7382E-01	1113.99584	.87002
.55680	.16000	.40198	.14199	.59497	.81042	7.3355E-01	1130.09004	.82580
.53213	.16250	.40149	.14337	.59843	.80493	7.9804E-01	1146.21956	.78445
.50890	.16500	.40101	.14475	.60186	.79932	8.6766E-01	1162.38265	.74574
.48702	.16750	.40053	.14611	.60528	.79358	9.4279E-01	1178.57872	.70948
.46637	.17000	.40006	.14747	.60866	.78770	1.0232E+00	1194.82756	.67547
.44689	.17250	.39961	.14881	.61203	.78172	1.1108E+00	1211.07899	.64354
.42848	.17500	.39916	.15015	.61537	.77559	1.2052E+00	1227.36094	.61355
.41108	.17750	.39872	.15148	.61869	.76933	1.3072E+00	1243.67210	.58534
.39461	.18000	.39828	.15280	.62199	.76293	1.4172E+00	1260.01127	.55879
.37901	.18250	.39785	.15411	.62526	.75638	1.5359E+00	1276.37731	.53378
.36423	.18500	.39743	.15541	.62852	.74967	1.6641E+00	1292.76908	.51021
.35022	.18750	.39702	.15670	.63175	.74281	1.8024E+00	1309.18543	.48797
.33692	.19000	.39661	.15799	.63497	.73578	1.9518E+00	1325.62526	.46696

TABLE III (cont)

X0290A X0290, PCJ=0.285, DCJ = 0.7707 10CT80 RHO = 1.89400
 POP PLOT, LN(RUN) = A1 + A2*LN(P-A3), A1 = -5.942871E+0, A2 = -2.923379E+00 A3 = 0.
 REACTION HUGONIOT, US = C + S*UP, C = 2.400000E+01 S = 2.500000E+00

RUN	P	V	UP	US	W	RATE	TEMPERATURE	TIME
.32428	.19250	.39622	.15926	.63816	.72858	2.1131E+00	1342.08745	.44712
.31228	.19500	.39582	.16053	.64134	.72120	2.2874E+00	1358.57091	.42835
.30086	.19750	.39544	.16180	.64449	.71365	2.4759E+00	1375.07457	.41060
.29008	.20000	.39505	.16305	.64763	.70590	2.6797E+00	1391.59733	.39378
.27966	.20250	.39468	.16430	.65075	.69793	2.9502E+00	1408.15879	.37785
.26980	.20500	.39431	.16554	.65385	.68984	3.1236E+00	1424.66982	.36275
.26041	.20750	.39395	.16677	.65693	.68145	3.3977E+00	1441.26979	.34841
.25145	.21000	.39359	.16800	.65999	.67290	3.5846E+00	1457.82778	.33481
.24290	.21250	.39324	.16922	.66304	.66404	4.0139E+00	1474.47725	.32188
.23474	.21500	.39289	.17043	.66607	.65501	4.3133E+00	1491.07649	.30959
.22694	.21750	.39254	.17163	.66908	.64571	4.6728E+00	1507.70385	.29791
.21948	.22000	.39221	.17283	.67208	.63616	5.0642E+00	1524.34207	.28679
.21235	.22250	.39187	.17402	.67506	.62634	5.4907E+00	1540.99016	.27620
.20552	.22500	.39155	.17521	.67802	.61623	5.9562E+00	1557.64716	.26611
.19899	.22750	.39122	.17639	.68197	.60583	6.4649E+00	1574.31208	.25650
.19273	.23000	.39090	.17756	.68391	.59512	7.0217E+00	1590.98395	.24733
.18674	.23250	.39059	.17873	.68682	.58410	7.6323E+00	1607.66184	.23858
.18099	.23500	.39028	.17989	.68973	.57273	8.3032E+00	1624.34478	.23023
.17548	.23750	.38997	.18105	.69262	.56101	9.0417E+00	1641.03184	.22225
.17019	.24000	.38967	.18220	.69549	.54893	9.8567E+00	1657.72210	.21463
.16511	.24250	.38937	.18334	.69835	.53652	1.0773E+01	1674.37411	.20734
.16023	.24500	.38908	.18448	.70120	.52366	1.1727E+01	1691.05472	.20037
.15554	.24750	.38878	.18561	.70403	.51038	1.2828E+01	1707.73266	.19371
.15104	.25000	.38850	.18674	.70685	.49665	1.4054E+01	1724.40657	.18732
.14671	.25250	.38821	.18786	.70965	.48246	1.5425E+01	1741.07500	.18121
.14254	.25500	.38793	.18898	.71244	.46778	1.6962E+01	1757.73651	.17535
.13854	.25750	.38766	.19009	.71522	.45258	1.8694E+01	1774.38957	.16973
.13468	.26000	.38738	.19119	.71799	.43684	2.0654E+01	1791.03263	.16435
.13096	.26250	.38712	.19230	.72074	.42053	2.2883E+01	1807.66409	.15919
.12738	.26500	.38685	.19339	.72348	.40360	2.5432E+01	1824.28228	.15423
.12393	.26750	.38659	.19448	.72621	.38604	2.8368E+01	1840.88548	.14947
.12061	.27000	.38633	.19557	.72892	.36780	3.1774E+01	1857.47191	.14490
.11740	.27250	.38607	.19665	.73163	.34885	3.5757E+01	1874.03973	.14051
.11431	.27500	.38581	.19773	.73432	.32913	4.0465E+01	1890.58751	.13629
.11133	.27750	.38556	.19880	.73700	.30861	4.6090E+01	1907.11234	.13223
.10845	.28000	.38532	.19987	.73967	.28723	5.2907E+01	1923.61256	.12833
.10566	.28250	.38507	.20093	.74232	.26493	6.1304E+01	1940.08600	.12458
.10298	.28500	.38483	.20199	.74497	.24166	7.1857E+01	1956.53041	.12096
.10038	.28750	.38459	.20304	.74760	.21736	8.5459E+01	1972.94340	.11749
.09787	.29000	.38435	.20409	.75023	.19195	1.0357E+02	1989.32250	.11414
.09545	.29250	.38412	.20514	.75284	.16535	1.2874E+02	2005.66511	.11091
.09310	.29500	.38388	.20618	.75544	.13748	1.6588E+02	2021.96850	.10780
.09083	.29750	.38366	.20721	.75803	.10825	2.2636E+02	2038.22978	.10480
.08864	.30000	.38343	.20825	.76061	.07736	3.3982E+02	2054.49698	.10191
.08651	.30250	.38320	.20927	.76319	.04503	6.2697E+02	2070.67647	.09912

TABLE III (cont)

X0290A X0290, PCJ=0.285, DCJ = 0.7707 10CT80 RHO = 1.84400
 LN(RATE) = C(1) + C(2)*P + ... + C(M+1)*(P**M)
 C(I=1,12) = -7.0669091872E+01 5.4704805945E+03 -2.1027371284E+05 4.7729141107E+06 -6.9948515921E+07
 6.9250697450E+08 -4.7375626849E+09 2.2417676762E+10 -7.2036423230E+10 1.4999723416E+11
 -1.8240619897E+11 9.8467173234E+10

PRESSURE	RATE	FIT	REL. ERROR
5.00000E-02	3.103456E-03	3.077053E-03	.000508
5.25000E-02	3.840523E-03	3.855041E-03	-.003780
5.50000E-02	4.708968E-03	4.743439E-03	-.007320
5.75000E-02	5.725193E-03	5.760406E-03	-.006150
6.00000E-02	6.907442E-03	6.927911E-03	-.002963
6.25000E-02	8.275304E-03	8.270973E-03	.000523
6.50000E-02	9.849069E-03	9.816977E-03	.003349
6.75000E-02	1.165432E-02	1.159506E-02	.005085
7.00000E-02	1.371306E-02	1.363556E-02	.005652
7.25000E-02	1.605277E-02	1.596957E-02	.005183
7.50000E-02	1.870209E-02	1.862857E-02	.003931
7.75000E-02	2.169180E-02	2.164424E-02	.002193
8.00000E-02	2.505499E-02	2.504837E-02	.000264
8.25000E-02	2.882716E-02	2.887309E-02	-.001593
8.50000E-02	3.304643E-02	3.315121E-02	-.003171
8.75000E-02	3.775365E-02	3.791686E-02	-.004323
9.00000E-02	4.299263E-02	4.320624E-02	-.004969
9.25000E-02	4.881029E-02	4.905853E-02	-.005086
9.50000E-02	5.525689E-02	5.551687E-02	-.004705
9.75000E-02	6.238626E-02	6.262937E-02	-.003897
1.00000E-01	7.025601E-02	7.044999E-02	-.002761
1.02500E-01	7.892779E-02	7.903940E-02	-.001414
1.05000E-01	8.846760E-02	8.846565E-02	.000022
1.07500E-01	9.894608E-02	9.880462E-02	.001430
1.10000E-01	1.104388E-01	1.101403E-01	.002703
1.12500E-01	1.230065E-01	1.225648E-01	.003591
1.15000E-01	1.367761E-01	1.361784E-01	.004369
1.17500E-01	1.518201E-01	1.510890E-01	.004816
1.20000E-01	1.682379E-01	1.674114E-01	.004912
1.22500E-01	1.861356E-01	1.852674E-01	.004664
1.25000E-01	2.056269E-01	2.047844E-01	.004097
1.27500E-01	2.268337E-01	2.260947E-01	.003258
1.30000E-01	2.498867E-01	2.493353E-01	.002206
1.32500E-01	2.749258E-01	2.746473E-01	.001013
1.35000E-01	3.021012E-01	3.021753E-01	-.000245
1.37500E-01	3.315742E-01	3.320680E-01	-.001489
1.40000E-01	3.635177E-01	3.644787E-01	-.002643
1.42500E-01	3.981177E-01	3.995663E-01	-.003639
1.45000E-01	4.355739E-01	4.374979E-01	-.004416
1.47500E-01	4.761011E-01	4.784488E-01	-.004931
1.50000E-01	5.199307E-01	5.226102E-01	-.005154

TABLE III (cont)

X0290A X0290, PCJ=0.285, DCJ = 0.7707
 LN(RATE) = C(1) + C(2)*P + ... + C(M+1)*(P**M)
 C(I=1,12) = -7.066909187E+01 5.4724805945E+03 -2.1027371284E+05 4.7729141107E+06 -6.9908515921E+07
 6.9250697450E+08 -4.7375626849E+09 2.2417676762E+10 -7.2036423230E+10 1.4999723416E+11
 -1.8249619897E+11 9.8467173234E+10

10CT80 RHO = 1.89400

PRESSURE	RATE	FIT	REL. ERROR
1.525000E-01	5.673116E-01	5.701883E-01	-.005071
1.550000E-01	6.185121E-01	6.214115E-01	-.004688
1.575000E-01	6.738218E-01	6.765342E-01	-.004025
1.600000E-01	7.335521E-01	7.358421E-01	-.003122
1.625000E-01	7.980425E-01	7.996581E-01	-.002024
1.650000E-01	8.676571E-01	8.683469E-01	-.001795
1.675000E-01	9.427923E-01	9.423208E-01	.001500
1.700000E-01	1.023216E+00	1.022044E+00	.001145
1.725000E-01	1.110771E+00	1.108038E+00	.002460
1.750000E-01	1.205247E+00	1.200884E+00	.003620
1.775000E-01	1.307191E+00	1.301226E+00	.004563
1.800000E-01	1.417198E+00	1.409774E+00	.005238
1.825000E-01	1.535918E+00	1.527303E+00	.005608
1.850000E-01	1.664057E+00	1.654655E+00	.005650
1.875000E-01	1.802390E+00	1.792734E+00	.005357
1.900000E-01	1.951764E+00	1.942511E+00	.004741
1.925000E-01	2.113109E+00	2.105016E+00	.003830
1.950000E-01	2.287446E+00	2.281338E+00	.002670
1.975000E-01	2.475898E+00	2.472624E+00	.001323
2.000000E-01	2.679707E+00	2.680079E+00	-.001139
2.025000E-01	2.90179E+00	2.904969E+00	.0015324
2.050000E-01	3.123642E+00	3.148631E+00	-.004000
2.075000E-01	3.397732E+00	3.412481E+00	-.004341
2.100000E-01	3.684614E+00	3.698043E+00	-.0031643
2.125000E-01	4.013930E+00	4.006974E+00	.001733
2.150000E-01	4.313316E+00	4.341115E+00	-.006445
2.175000E-01	4.672839E+00	4.702541E+00	-.006356
2.200000E-01	5.064187E+00	5.093643E+00	-.005817
2.225000E-01	5.490698E+00	5.517216E+00	-.004829
2.250000E-01	5.956154E+00	5.976368E+00	-.003427
2.275000E-01	6.464852E+00	6.475657E+00	-.001671
2.300000E-01	7.021690E+00	7.019233E+00	.000351
2.325000E-01	7.632312E+00	7.613018E+00	.002528
2.350000E-01	8.303161E+00	8.263887E+00	.004730
2.375000E-01	9.041720E+00	8.980089E+00	.006816
2.400000E-01	9.856674E+00	9.771464E+00	.008645
2.425000E-01	1.073597E+01	1.064970E+01	.008035
2.450000E-01	1.172721E+01	1.162060E+01	.008409
2.475000E-01	1.282804E+01	1.272435E+01	.008084
2.500000E-01	1.405429E+01	1.395578E+01	.007009

TABLE III (cont)

X_{0290A} X_{0290} , $PCJ=0.285$, $DCJ = 0.7707$ 10CTAN $RHO = 1.89440$
 $LN(RATE) = C(1) + C(2)*P + \dots + C(M+1)*(P**M)$
 $C(I=1,12) =$ $-7.0669091872E+01$ $5.4704805945E+03$ $-2.1027371284E+05$ $4.7729141107E+06$ $-6.9908515921E+07$
 $6.9250697450E+08$ $-4.7375626849E+09$ $2.2417676762E+10$ $-7.2036423230E+10$ $1.4999723410E+11$
 $-1.8249619897E+11$ $9.8467173234E+10$

PRESSURE	RATE	FIT	REL. ERROR
2.525000E-01	1.542482E+01	1.534480E+01	.005187
2.550000E-01	1.696220E+01	1.691663E+01	.002691
2.575000E-01	1.869409E+01	1.870025E+01	-.000329
2.600000E-01	2.065377E+01	2.072096E+01	-.003641
2.625000E-01	2.288266E+01	2.304120E+01	-.006928
2.650000E-01	2.543236E+01	2.568177E+01	-.009807
2.675000E-01	2.836811E+01	2.870408E+01	-.011843
2.700000E-01	3.177350E+01	3.217382E+01	-.012599
2.725000E-01	3.575744E+01	3.617545E+01	-.011690
2.750000E-01	4.046462E+01	4.082320E+01	-.008862
2.775000E-01	4.609049E+01	4.627979E+01	-.004107
2.800000E-01	5.290721E+01	5.278820E+01	.002249
2.825000E-01	6.130387E+01	6.072620E+01	.009423
2.850000E-01	7.185707E+01	7.070210E+01	.016073
2.875000E-01	8.545900E+01	8.372908E+01	.024243
2.900000E-01	1.035671E+02	1.015591E+02	.019389
2.925000E-01	1.287353E+02	1.273626E+02	.014663
2.950000E-01	1.658827E+02	1.672158E+02	-.000036
2.975000E-01	2.263640E+02	2.336337E+02	-.032115
3.000000E-01	3.398181E+02	3.548103E+02	-.044118
3.025000E-01	6.269734E+02	6.016798E+02	.040342

TABLE IV
PBX 9502 SHOCK INITIATION DATA

	Booster ^a	Attenuator ^b	Ratio Atten./HE Thickness	U_{fs} ^c (mm/ μ s)	Density (g/cm ³)	U_s ^d (mm/ μ s)	U_p ^e (mm/ μ s)	P_e (GPa)	V/V_0 ^e	x^*f (mm)	t^*f (μ s)
<u>X0290</u>											
E-4105	P8-51T	PMMA	0.25	3.73	1.897	5.80	1.47	16.2	0.747	4.64	0.756
E-4106	P8-25T	PMMA	0.95	3.14	1.898	5.24	1.24	12.3	0.763	12.78	2.243
E-4121	P8-51T	PMMA	0.38	3.57	1.902	5.45	1.43	14.8	0.738	5.88	0.994
E-4122	P8-25T	PMMA	1.50	2.77	1.896	4.80	1.10	10.0	0.771	15.38	2.893
<u>PBX 9502</u>											
E-4696	P12-51T	PMMA	0.24	3.85	1.893	5.32	1.60	16.1	0.700	2.24	0.38
E-4738	P8-51T	PMMA	0.25	4.01	1.893	5.84	1.61	17.8	0.725	2.30	0.40
E-4737	P8-51T	PMMA	0.25	4.09	1.896	5.40	1.71	17.5	0.683	2.73	0.49
B-8425	P8-51T	PMMA	0.25	3.81	1.893	5.78	1.51	16.6	0.738	4.28	0.71
E-4718	P8-25T	PMMA	0.60	3.37	1.897	5.05	1.38	13.2	0.727	6.55	1.20
E-4729	P8-51C	SS	0.45	1.62	1.892	5.41	1.29	13.2	0.762	6.96	1.24
B-8513	P8-51C	SS	0.50	1.46	1.892	5.00	1.18	11.1	0.765	11.41	2.11
B-8424	P12-25T	PMMA	1.50	2.89	1.894	4.90	1.16	10.7	0.764	12.5	2.35
B-8557	P8-51C	SS	0.50	1.38	1.895	4.92	1.11	10.4	0.774	13.7	2.59
E-4695	P12-51B	PMMA	0.24	2.63	1.893	4.72	1.05	9.37	0.778	16.9	3.40
E-4741	P12-51B	PMMA	0.36	2.66	1.895	4.55	1.08	9.33	0.762	20.8	4.24
B-8549	P12-51B	Dural	0.37	1.57	1.895	4.99	1.01	9.51	0.798	22.6	4.33
B-8534	P12-51B	PMMA	0.48	2.54	1.895	4.67	1.01	8.93	0.784	23.7	4.74
B-8553	P12-51B	Dural	0.68	1.49	1.895	4.58	0.98	8.51	0.786	24.9	5.08
B-8569 ^g	P12-51T	SS	0.37	1.08	1.895	4.46	0.88	7.48	0.802	39.9	8.48
B-8577 ^g	P12-51T	SS	0.36	1.09	1.894	4.61	0.89	7.75	0.807	30.5	6.35
B-8511	P8-51B	PMMA	0.36	2.52	1.894	4.58	1.01	8.76	0.780	19.1	5.43
E-4739	P12-51C-25S	PMMA	0.22	2.10	1.895	4.40	0.82	6.86	0.813	>55	>12.5
B-8542	P12-51C-17S	PMMA	0.32	2.05	1.894	4.43	0.77	6.69	0.820	>55	>12.8
B-8514	P12-51T-19S	PMMA	0.25	1.70	1.894	4.10	0.66	5.14	0.838	>55	>13.3
<u>WX-7 Data</u>											
15-1323	P8-510C	Dural	0.25	3.43	1.885	7.19	2.02	27.4	0.719	0.68	0.104
15-1325	P8-510C	Dural	0.25	3.50	1.885	7.39	2.05	28.6	0.727	0.63	0.102
15-1328	P8-510C	Dural	0.25	3.34	1.885	7.11	1.98	26.5	0.722	0.72	0.090
15-1324	P8-51C	Dural	0.25	3.03	1.885	6.24	1.86	21.9	0.702	1.49	0.225
15-1326	P8-51C	Dural	0.25	3.04	1.885	6.58	1.83	22.7	0.722	1.43	0.213
15-1355	P8-51T	Dural	0.25	2.54	1.885	5.69	1.59	17.0	0.721	3.92	0.661
15-1357	P8-51T	Dural	0.25	2.43	1.885	5.41	1.54	15.7	0.715	4.59	0.774
15-1358	P8-51T	Dural	0.50	2.16	1.885	5.21	1.38	13.5	0.735	8.50	1.51
15-1360	P8-51T	Dural	0.50	2.20	1.885	5.27	1.40	13.9	0.734	7.96	1.41
15-1354	P8-51B	Dural	0.25	1.67	1.885	4.61	1.10	9.5	0.761	-----	-----

^aAbbreviated code for booster system (P8 = P081 plane wave lens, P12 = P120 wave lens, 51C = 51-mm Composition B, 25T = 25-mm TNT, xxOC = xx-mm Octal, xxB = xx-mm Baratol, and xxS = xx-mm Stainless steel (type 304)).

^bMaterial in final attenuator plate (driver) adjacent to the acceptor explosive. PMMA is polymethylmethacrylate, Dural is 6061 Dural, and SS is stainless steel (type 304).

^cFree-surface velocity of the driver material. For the M-3 shots this variable was measured using the reflected-wire technique.

^dValue for the shock velocity extrapolated to the point of entry of the shock wave into the explosive.

^eParticle velocity, pressure, and compression obtained by matching the particle velocity and pressure of the driver and the explosive at the interface.

^fDistance and time to the transition to detonation measured from the shot record.

^gThere is no explanation for the significantly lower measured detonation velocity for these shots.

The pressure contours are shown in Fig. 11, and the calculated initial plate movement and the experimental reflectance times from a 1.27-mm air gap between the Dural plate and a Plexiglas block are shown in Fig. 12.

The calculated and experimental Dural plate positions under the axis of the detonator are shown in Fig. 13, and the calculated and experimental plate velocities are shown in Fig. 14.

VI. PBX 9502 POP PLOT DATA

The Pop plot data for PBX 9502 are shown in Fig. 15 and Table IV. Although there is considerable spread in the data, the Pop plot used in Ref. 1 for X0290 adequately describes the data. The WX-7 data were obtained by W. L. Seitz.

VII. CONCLUSIONS

The available performance data for PBX 9502 indicate that the BKW or gamma-law isentropic is adequate to describe the behavior of the detonation products. The buildup of detonation characteristic of many explosives was not observed for PBX 9502.

The rate of energy release from shocked, but not detonated, PBX 9502 may be described using the multiple-shock Forest Fire decomposition model.

REFERENCES

1. C. L. Mader, Numerical Modeling of Detonations (University of California Press, Berkeley, 1979).
2. Charles L. Mader and Richard Dick, "Explosive Desensitization by Preshocking," in Combustion and Detonation Processes, Internationale Jahrestagung, June 27-29, 1979 (Karlsruhe, Bundesrepublik Deutschland, 1979), pp. 569-579.
3. Allen L. Bowman, James D. Kershner, and Charles L. Mader, "A Numerical Model of the Gap Test," Los Alamos Scientific Laboratory report LA-8408 (October 1980).
4. Charles L. Mader and George H. Pimbley, "Jet Initiation of Explosives," Los Alamos National Laboratory report LA-8647 (February 1981).
5. Charles L. Mader and James D. Kershner, "Three-Dimensional Modeling of Triple-Wave Initiation of Insensitive Explosives," Los Alamos National Laboratory report LA-8655 (February 1981).
6. Charles L. Mader, "Numerical Modeling of Insensitive High-Explosive Initiators," Los Alamos Scientific Laboratory report LA-8437-MS (July 1980).
7. B. G. Craig, J. N. Johnson, C. L. Mader, and G. F. Lederman, "Characterization of Two Commercial Explosives," Los Alamos Scientific Laboratory report LA-7140 (May 1978).

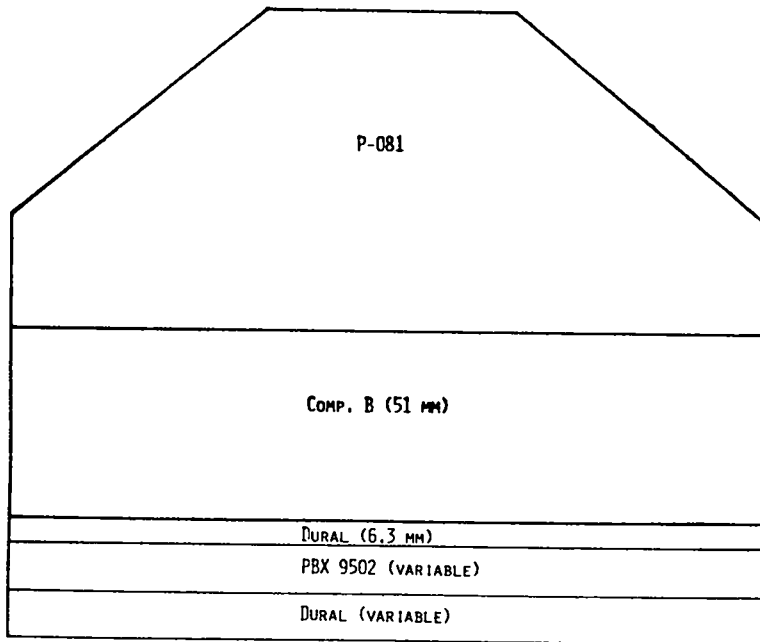


Fig. 1.
Experimental configuration
for Fig. 2.

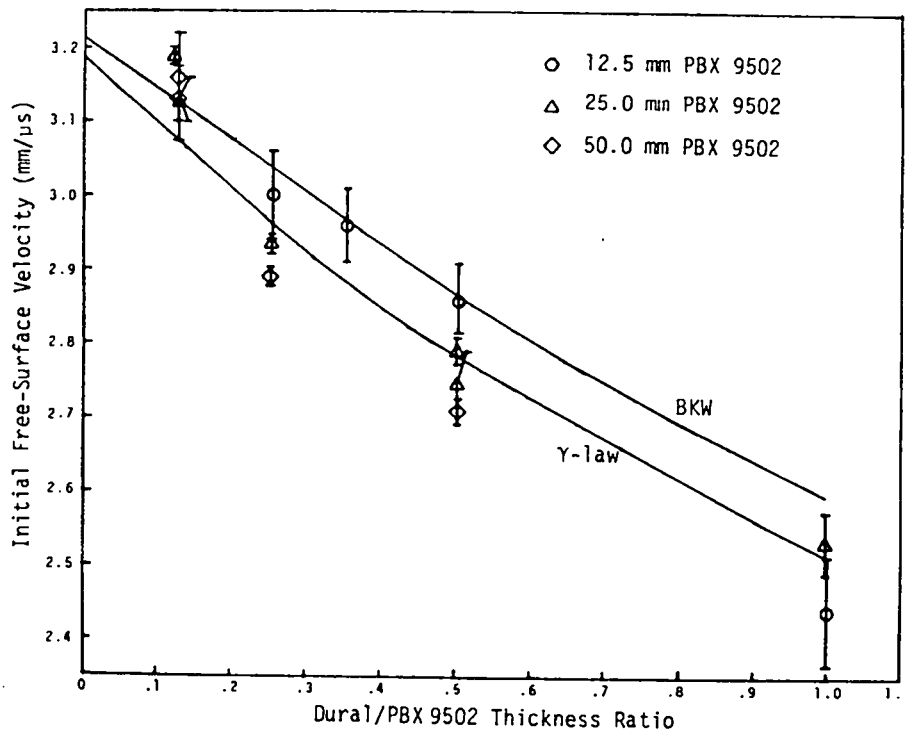


Fig. 2.
Dural free-surface ve-
locity as a function of
Dural plate thickness/
PBX 9502 thickness.

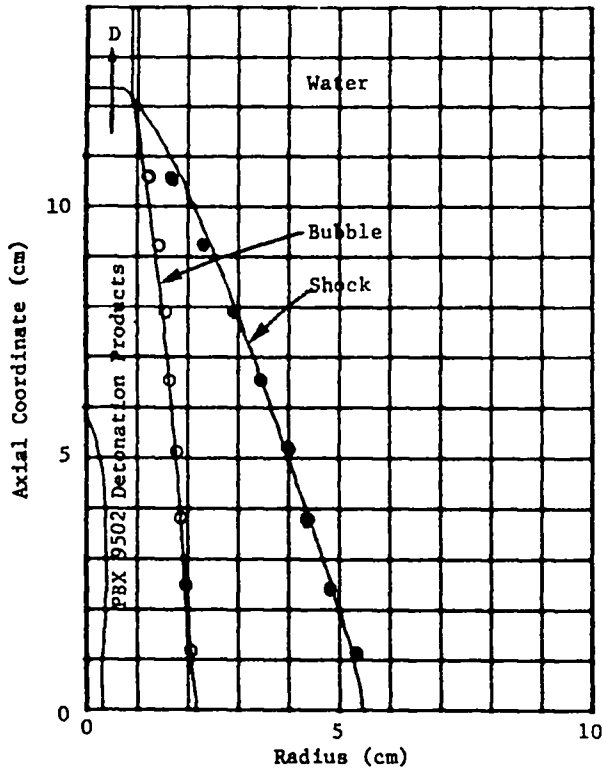


Fig. 3.

Aquarium test data for PBX 9502 compared to 2DL calculation using BKW isentrope.

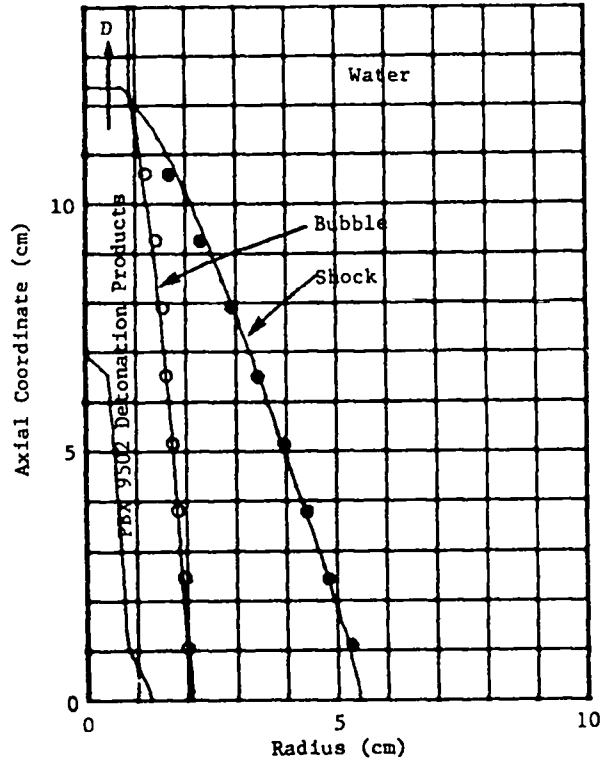


Fig. 4.

Aquarium test data for PBX 9502 compared to 2DL calculation using gamma-law isentrope.

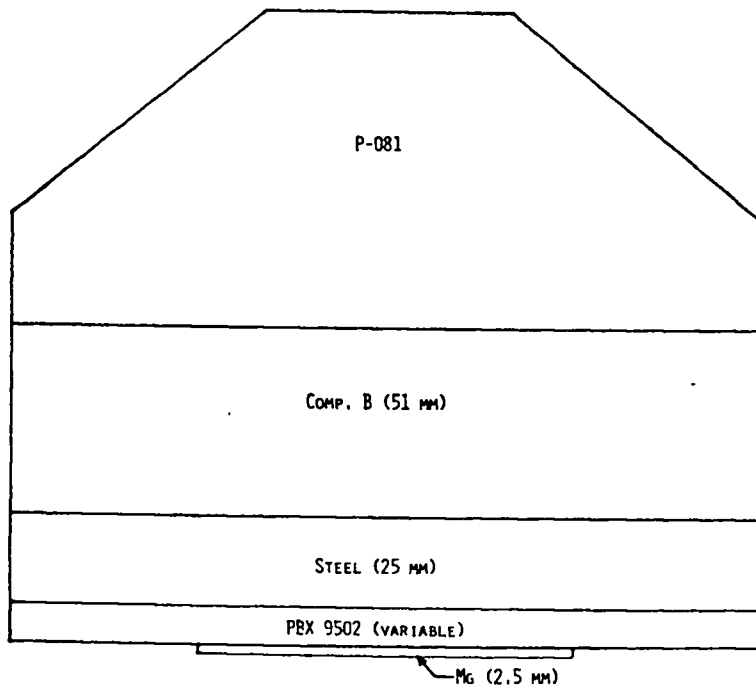


Fig. 5.
Experimental configuration for Figs. 6-10.

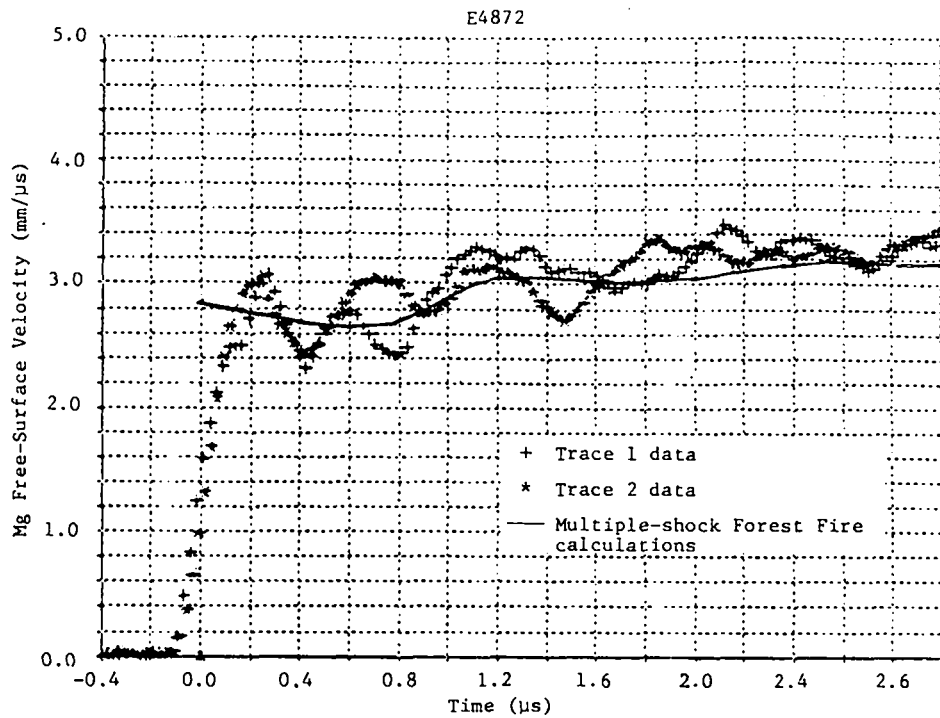


Fig. 6.
Magnesium free-surface velocity vs time for 4.52 mm PBX 9502 shocked to 135 kbar.

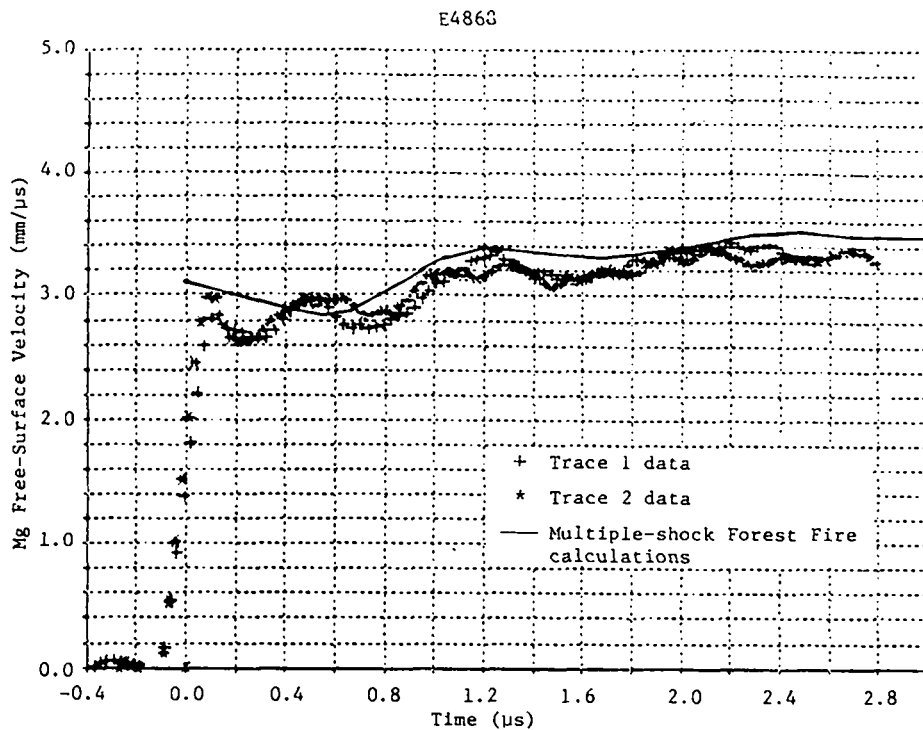


Fig. 7.
Magnesium free-surface velocity vs time for 7.57 mm PBX 9502 shocked to 135 kbar.

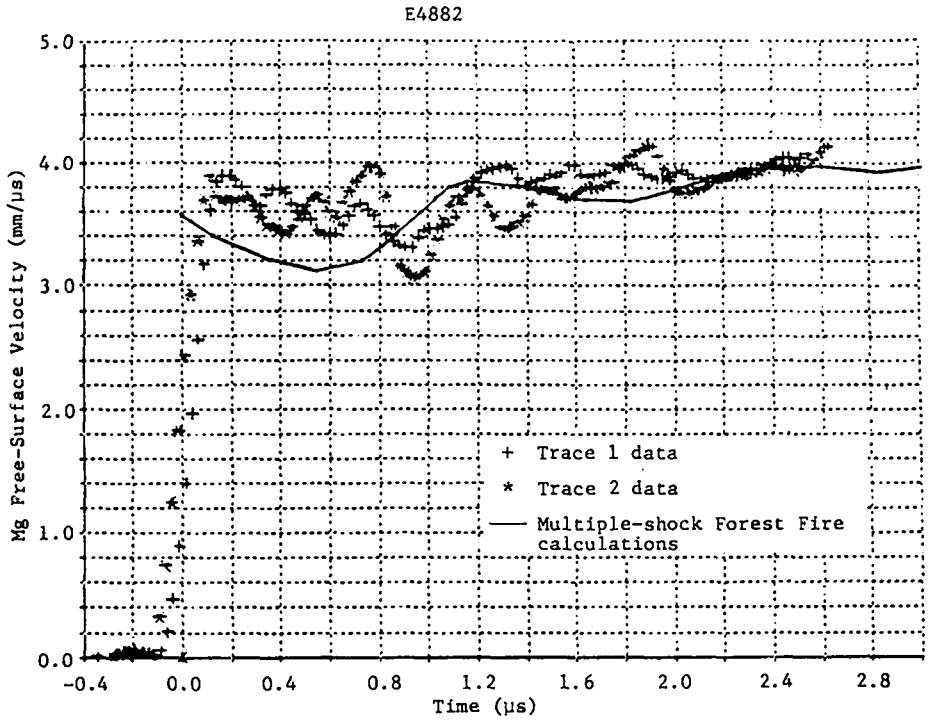


Fig. 8.
Magnesium free-surface velocity vs time for 10.51 mm PBX 9502 shocked to 135 kbar.

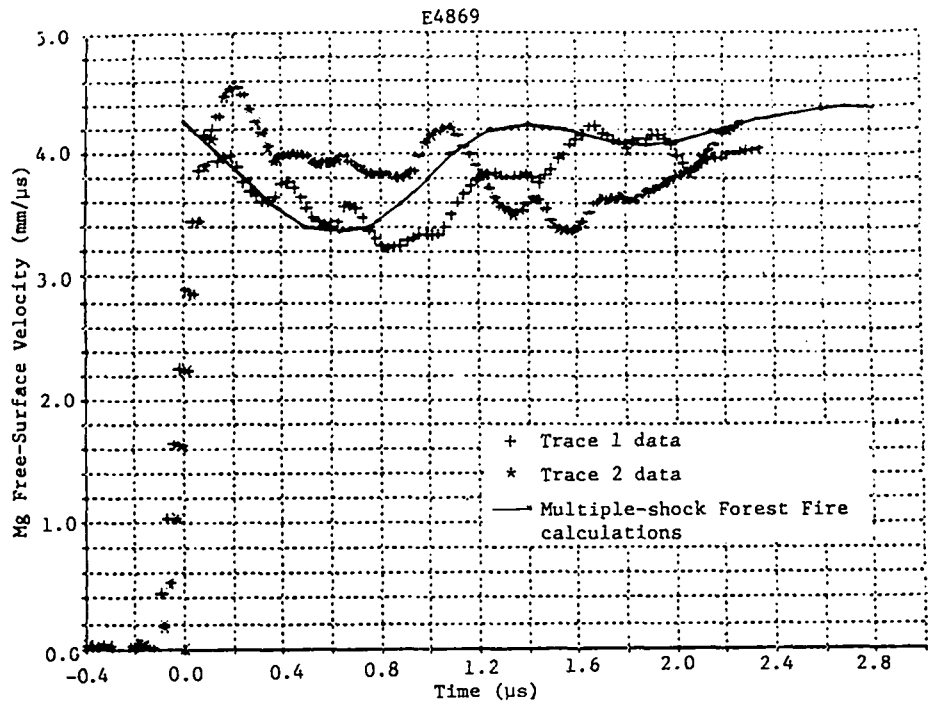


Fig. 9.
Magnesium free-surface velocity vs time for 17.50 mm PBX-9502 shocked to 135 kbar.

E4885

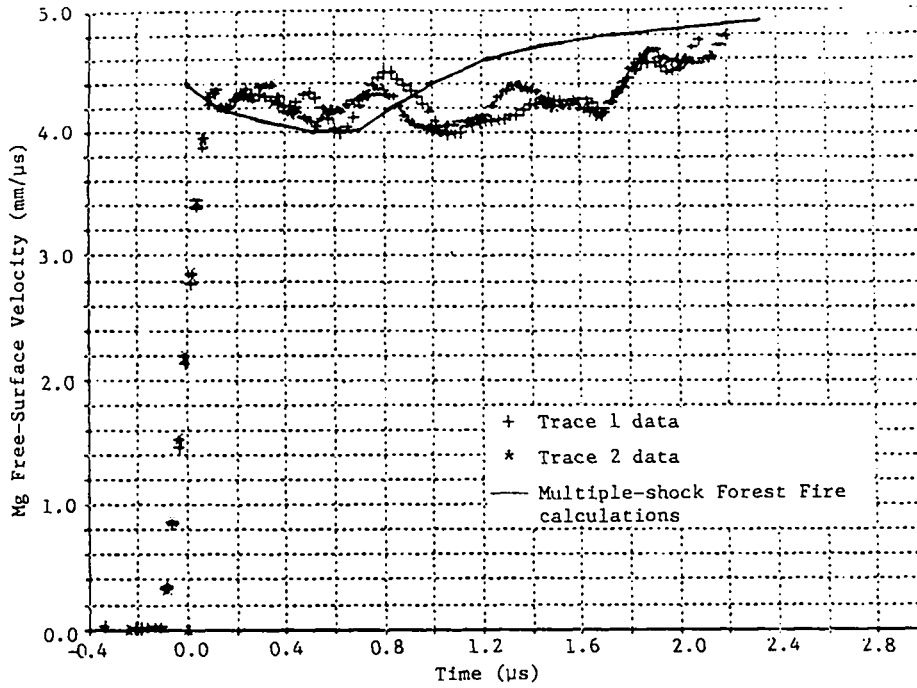


Fig. 10.

Magnesium free-surface velocity vs time for 49.97 mm PBX 9502 shocked to 135 kbar.

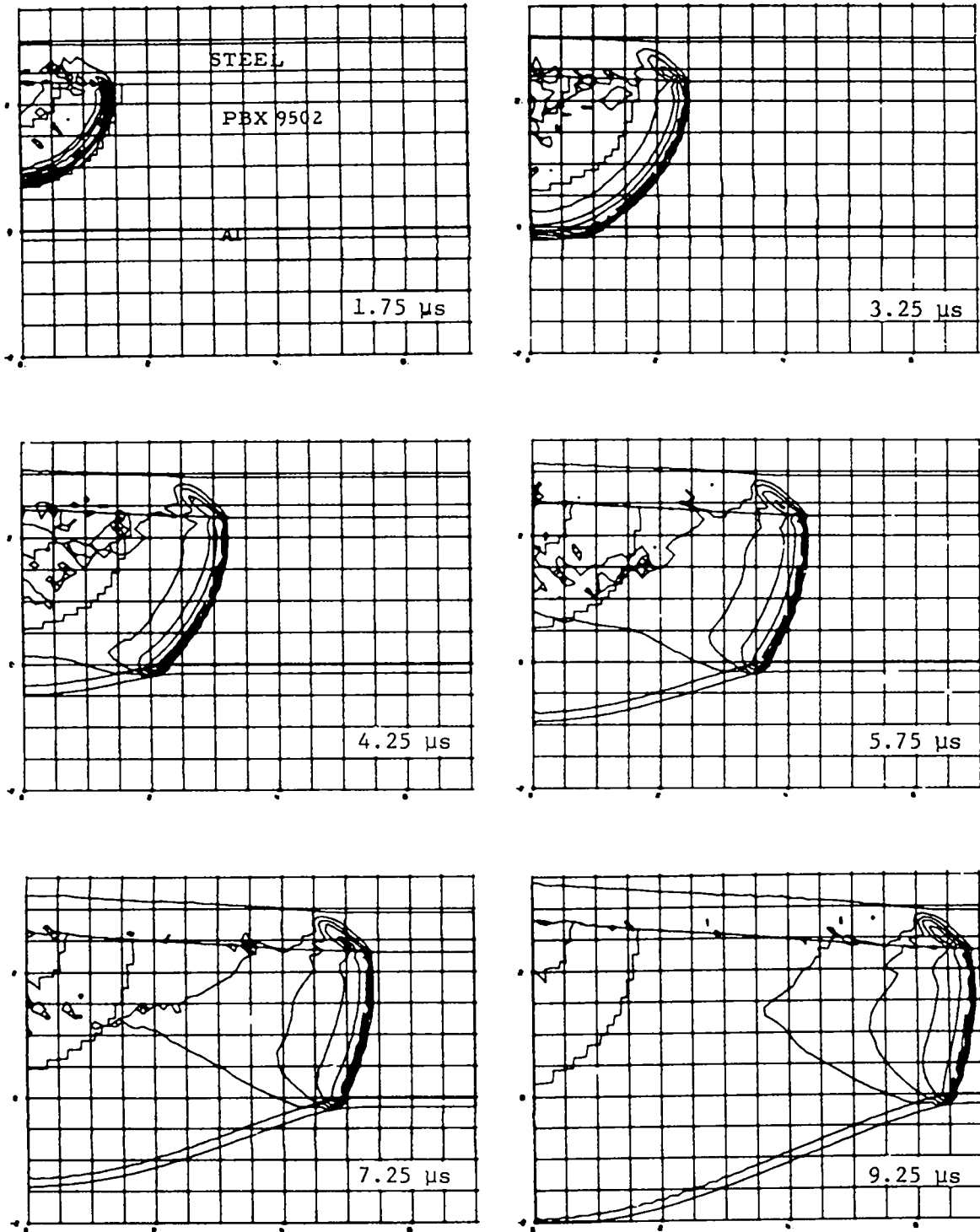


Fig. 11.
 Pressure contours at various times for a hemispheric initiator of 16-mm-radius X0351 initiating PBX 9502 and driving a 6.35-mm steel plate.

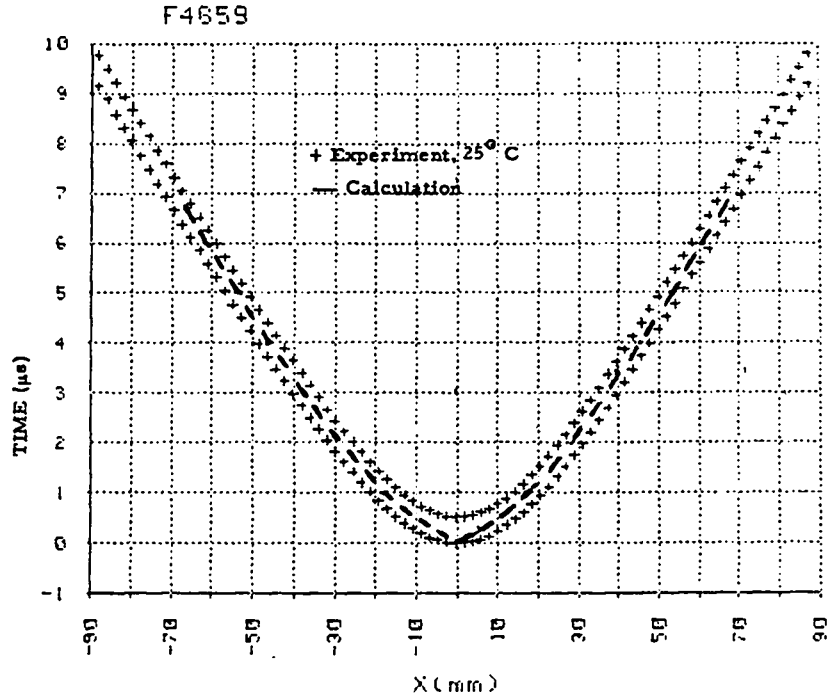


Fig. 12.

The time to initial movement of the aluminum plate as a function of distance from detonator axis.

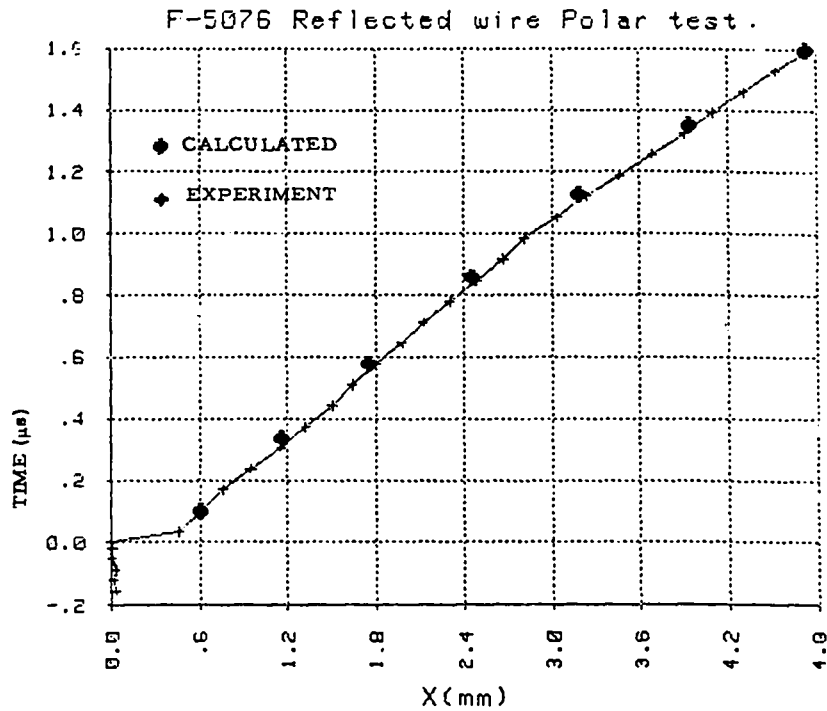


Fig. 13.

The calculated and experimental Dural plate position under the detonator axis as a function of time.

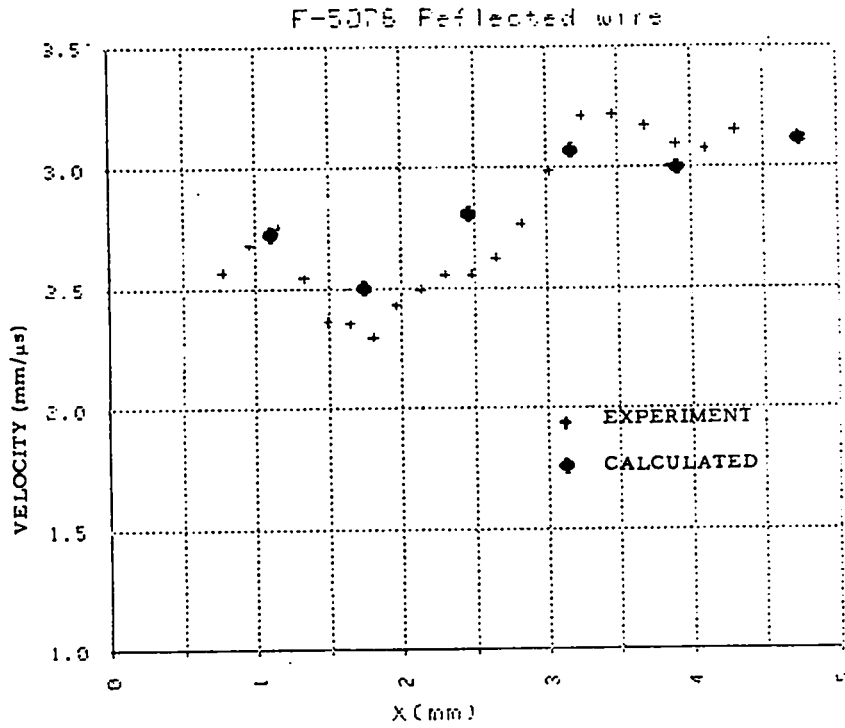


Fig. 14.

The calculated and experimental Dural plate velocity under the detonator axis as a function of time.

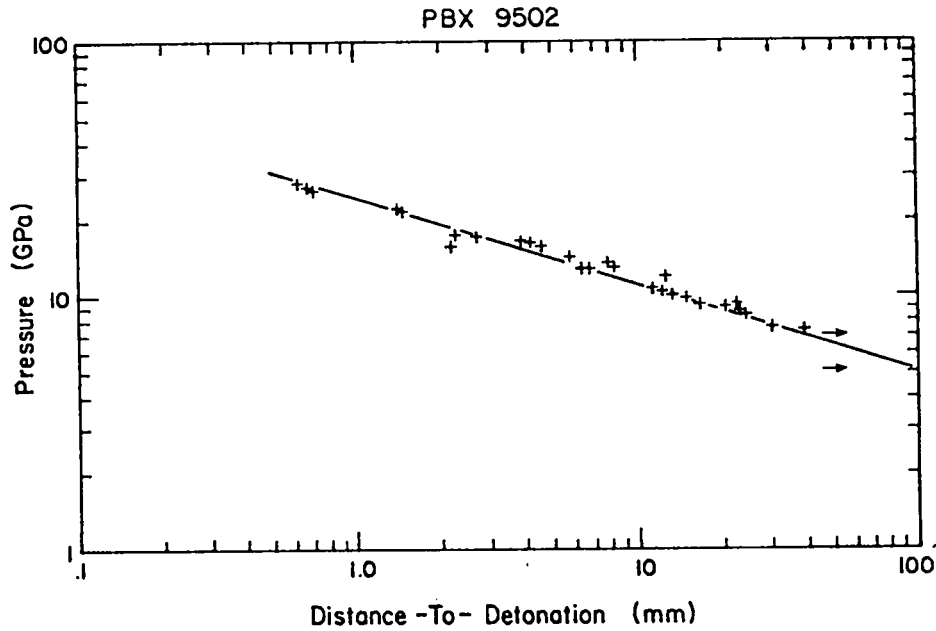


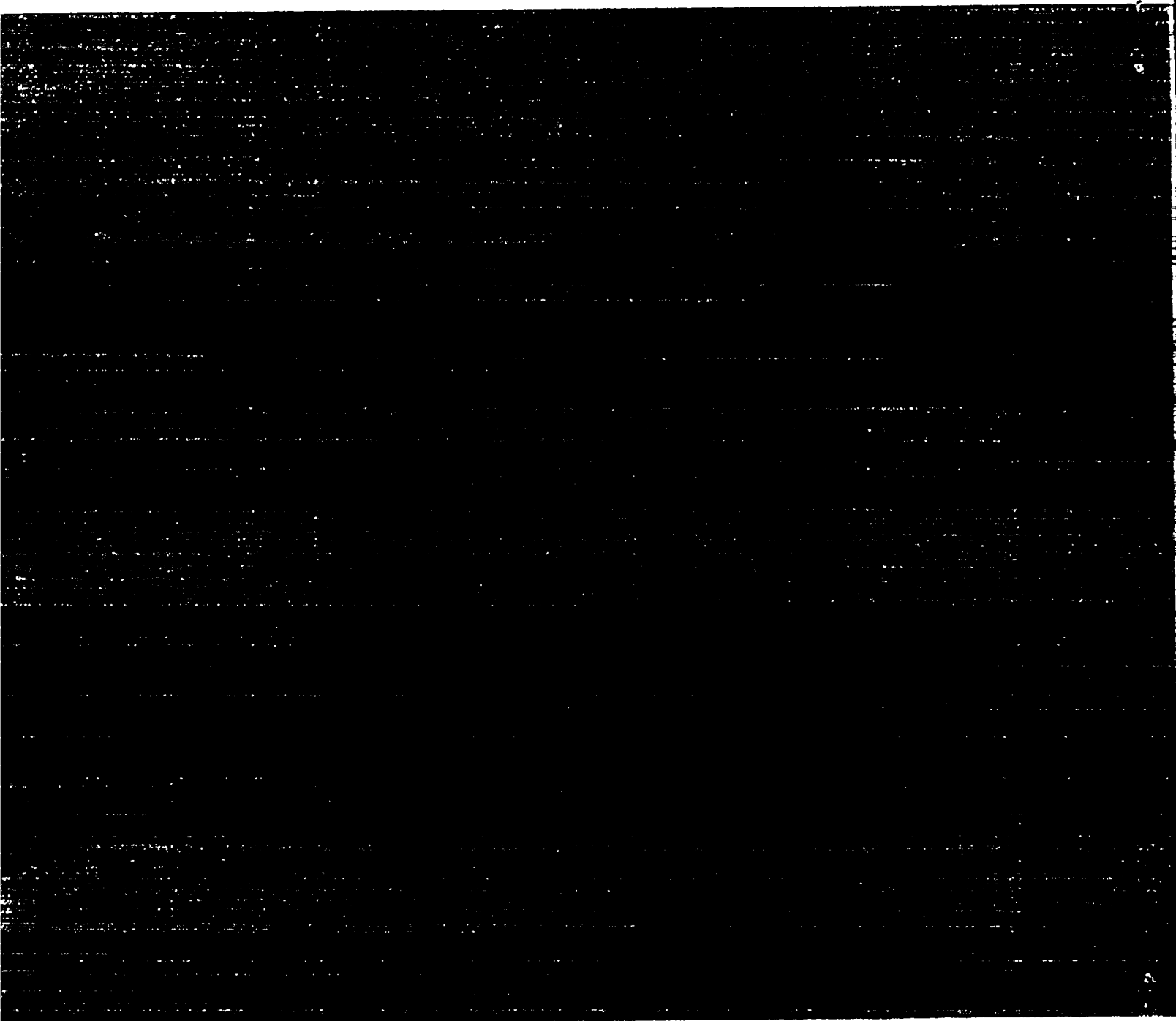
Fig. 15.

The Pop plot for PBX 9502.

Printed in the United States of America
 Available from
 National Technical Information Service
 US Department of Commerce
 5285 Port Royal Road
 Springfield, VA 22161
 Microfiche \$3.50 (A01)

Page Range	Domestic Price	NTIS Price Code	Page Range	Domestic Price	NTIS Price Code	Page Range	Domestic Price	NTIS Price Code	Page Range	Domestic Price	NTIS Price Code
001-025	\$ 5.00	A02	151-175	\$11.00	A08	301-325	\$17.00	A14	451-475	\$23.00	A20
026-050	6.00	A03	176-200	12.00	A09	326-350	18.00	A15	476-500	24.00	A21
051-075	7.00	A04	201-225	13.00	A10	351-375	19.00	A16	501-525	25.00	A22
076-100	8.00	A05	226-250	14.00	A11	376-400	20.00	A17	526-550	26.00	A23
101-125	9.00	A06	251-275	15.00	A12	401-425	21.00	A18	551-575	27.00	A24
126-150	10.00	A07	276-300	16.00	A13	426-450	22.00	A19	576-600	28.00	A25
									601-up	†	A99

†Add \$1.00 for each additional 25-page increment or portion thereof from 601 pages up



Los Alamos